Structure–Function Relationships in the 47-kDa Antenna Protein and Its Complex with the Photosystem II Reaction Center Core: Insights from Picosecond Fluorescence Decay Kinetics and Resonance Raman Spectroscopy†

Julio C. de Paula,*,‡ Ann Liefshitz,‡ Sarina Hinsley,‡ Wei Lin,‡ Vikas Chopra,‡ Kathryn Long,‡ Scott A. Williams,§ Scott Betts,∥ and Charles F. Yocum∥

Department of Chemistry, Haverford College, Haverford, Pennsylvania 19041, Regional Laser and Biotechnology Laboratories, The University of Pennsylvania, Philadelphia, Pennsylvania 19104, and Department of Biology, The University of Michigan, Ann Arbor, Michigan 48109

Received May 3, 1993; Revised Manuscript Received November 16, 1993⊗

ABSTRACT: We report the fluorescence decay kinetics and the vibrational properties of chlorophyll *a* bound to the 47-kDa antenna protein (CP47) of spinach photosystem II. The chlorophyll fluorescence of CP47 samples decays with four lifetimes (τ = 75.8 ps, 1.05 ns, 3.22 ns, and 5.41 ns). The 75.8-ps and 3.22-ns components are associated with chlorophyll *a* bound to relatively intact centers, the 1.05-ns component corresponds to chlorophyll bound to centers that are slightly perturbed, and the the 5.41-ns phase probably originates from centers that are severely denatured. The resonance Raman spectrum of CP47 at 441.6 nm (this work) and at 406.7 nm [de Paula, J. C., Ghanotakis, D. F., Bowlby, N. R., Dekker, J. P., Yocum, C. F., & Babcock, G. T. (1990) in *Current Research in Photosynthesis* (Baltscheffsky, M., Ed.), Vol. I, pp 643–646, Kluwer Academic Publishers, Dordrecht, The Netherlands] shows heterogeneity in the C=O stretching region. This part of the spectrum monitors the environment of the keto group at position 9 of the chlorophyll *a* molecule. We show that several structurally distinct pools of chlorophyll *a* are bound to CP47. Four of these may be distinguished by their C_9=O stretching frequencies ($\nu_{C=O}$ = 1670, 1688, 1693, and 1701 cm^{-1}). By analyzing the resonance enhancement pattern of these modes, we ascribe the 1693-cm^{-1} vibration to denatured centers. Of the remaining populations, we propose that the 1670-cm^{-1} vibration is consistent with a hydrogen bond between the C_9=O group of chlorophyll *a* and the protein. We elaborate on the role of this chromophore–protein interaction in the mechanism of energy transfer within the 47-kDa antenna protein.

In photosynthesis, solar energy is collected by tetrapyrrole or polyene chromophores bound to so-called antenna proteins. Within picoseconds, the excitation energy is transferred to reaction center complexes, where ultrafast electron transfer creates a stable transmembrane electrical potential. Much of our knowledge of photosynthetic energy transfer comes from biochemical, crystallographic, and spectroscopic studies of photosynthetic bacteria [reviewed by Hawthornthwaite and Cogdell (1991), Deisenhofer and Michel (1991), and Sundström and van Grondelle (1991)]. As bacterial photosynthesis may not provide a universal archetype for solar energy conversion systems, it is important to determine the correlation between structure and function in the chlorophyll-binding proteins of plants, as well.

Plants have two reaction centers that operate in series, forming two photosystems. Light-induced electron transfer through photosystems I and II results in the oxidation of H_2O and reduction of $NADP^+$,[1] with the concomitant synthesis of ATP. Our efforts are directed at understanding energy transfer in photosystem II (PSII).

The PSII reaction center core consists of polypeptides with molecular masses of 32 kDa (D1), 34 kDa (D2), 9 kDa, and 4.5 kDa (Nanba & Satoh, 1987; Akabori et al., 1988; Ghanotakis et al., 1989). The first two bind at least six chlorophyll *a* molecules, two pheophytin *a* molecules, one or two β-carotene molecules, and no quinones (Kobayashi et al., 1990). The latter two polypeptides comprise cytochrome *b*-559, a heme protein that may protect PSII against photoinhibition (Thompson & Brudvig, 1988). The D1/D2/cytochrome *b*-559 complex, hereafter referred to as the PSII core, is the smallest unit capable of photoinduced electron transfer characteristic of PSII (Wasielewski et al., 1989a,b).

Photochemistry of the PSII core has been studied extensively by a variety of ultrafast spectroscopic techniques. Excitation of a chlorophyll species called P680 to its first excited singlet state (P680*) leads to the transfer of an electron to a pheophytin (Pheo) molecule within picoseconds. There is some controversy related to the kinetics of this event. Working at room temperature, Wasielewski et al. (1989a) report oxidation of P680 within 3 ps, whereas Hastings et al. (1992) and McCauley et al. (1992) observe photoreduction of Pheo with time constants of 21 and 13 ps, respectively.

† J.d.P. acknowledges funding by the Donors of the Petroleum Research Fund, administered by the American Chemical Society (Grant 23299-GB3), the Olin Charitable Trust of the Research Corporation (Grant C-3007), and the Howard Hughes Medical Institutes. C.F.Y. acknowledges funding by the National Science Foundation (Grant DCB89-04075). The Regional Laser and Biotechnology Laboratories are funded by the National Institutes of Health (Grant RR01348).

‡ Haverford College.
§ The University of Pennsylvania.
∥ The University of Michigan.

⊗ Abstract published in *Advance ACS Abstracts,* January 15, 1994.

[1] Abbreviations: ATP, adenosine triphosphate; Chl, chlorophyll; CP47, chlorophyll *a* binding protein associated with energy transfer in photosystem II and having an apparent molecular mass of 47 kDa; D1 and D2, polypeptides that make up the reaction center of photosystem II; Mes, 2-(*N*-morpholino)ethanesulfonic acid; $NADP^+$, oxidized form of nicotinamide adenine dinucleotide phosphate; P680, primary electron donor of PSII; Pheo, pheophytin; PSII, photosystem II; λ_Q, wavelength of the lowest energy π–π^* electronic transition [Q_y(0–0) transition] of chlorophylls; $\nu_{C=O}$, frequency of the stretching mode associated with the C_9 keto group of chlorophyll *a*.

0006-2960/94/0433-1455$04.50/0

In the absence of bound plastoquinones, which accept electrons from $Pheo^-$ in intact PSII, the $P680^+Pheo^-$ state decays via charge recombination, yielding either the excited singlet state (P680*Pheo) or an intermediate triplet state, ^{3}P680Pheo (Takahashi et al., 1987). The reformation of P680* leads to long-lived chlorophyll fluorescence whose decay kinetics correspond to the back electron transfer time. This process has been studied extensively by picosecond fluorescence (Mimuro et al., 1988; Govindjee et al., 1990; Booth et al., 1991; Roelofs et al., 1991) and absorption (Takahashi et al., 1987; Hansson et al., 1988) methods, yielding at least two models for charge recombination in the PSII core. Some reports assign a discrete lifetime of approximately 30–40 ns to the $P680^+Pheo^- \rightarrow$ P680*Pheo $\rightarrow$ P680Pheo reaction sequence (Mimuro et al., 1988; Roelofs et al., 1991). On the other hand, Govindjee et al. (1990) proposed the existence of a continuous distribution of charge recombination times from 5 to 20 ns. Booth et al. (1991) and Roelofs et al. (1991) also observed chlorophyll fluorescence components decaying within ~4 ns but assigned this component to denatured centers, where chlorophyll has become disconnected from energy or electron transfer events. It is unclear why there is so much variability in the published fluorescence decay data of PSII cores. It is worth pointing out, however, that all four of the groups discussed above worked with PSII cores that were prepared by solubilization with Triton X-100. This procedure is known to yield product that is particularly unstable toward exposure to light (Akabori et al., 1988).

There are two kinds of antenna proteins associated with PSII [reviewed by Thornber et al. (1991) and Bricker (1990)]. A peripheral antenna with an approximate molecular mass of 28 kDa binds both chlorophyll *a* and chlorophyll *b*. This protein may be removed easily from PSII membranes by treatment with mild, nonionic detergents (Ghanotakis & Yocum, 1986). More strongly associated with the reaction center core are two chlorophyll *a*-binding antennas with apparent molecular masses of 43 and 47 kDa. Of these, the 43-kDa antenna protein is more loosely bound to the reaction center than the 47-kDa protein (Ghanotakis et al., 1989).

In addition to acting as a carrier of excitation energy, the 47-kDa antenna protein (hereafter referred to as CP47) may also play a structural role in PSII (Bricker, 1990). Vermaas et al. (1987) have shown that mutants of the cyanobacterium *Synechocystis* sp. PCC 6803 lacking CP47 did not assemble a functional PSII complex, as judged by the abolition of O_2-evolution activity. Other lines of evidence indicate that electron transfer to P680 is affected by binding of CP47. Petersen et al. (1990) have shown that photooxidation of tyrosine-161 of the D1 polypeptide occurs only in PSII reaction center complexes where CP47 is present. Tyr-161, also known as Y_z, is the immediate electron donor to P680.

CP47 binds 20–25 chlorophyll *a* molecules (de Vitry et al., 1984), β-carotene molecules [at a chlorophyll:carotene ratio of 10:1 (Akabori et al., 1988)], no pheophytins, and no quinones. Although the sequence of the protein is known (Vermaas et al., 1987) and a folding pattern has been proposed, the spatial arrangement of the bound pigments has not been determined. This information is crucial to our understanding of the mechanisms of energy transfer mediated by CP47. The transmembrane regions of the protein have a total of 14 histidine residues, whose imidazole side chains are known to be good ligands of chlorophyll in bacterial chlorophyll–protein complexes (Deisenhofer & Michel, 1991). However, backbone carbonyls and other residues, such as tyrosine, glutamine, and asparagine, may also ligate to chlorophyll. Indeed, ligands other than histidine must be invoked to reconcile the sequence data with pigment stoichiometry. In short, a consideration of the amino acid sequence is not sufficient to yield a map of the binding sites for chlorophyll *a* in CP47.

Spectroscopic studies have provided sketchy details of the organization of pigments in CP47. Van Dorssen et al. (1987) measured the absorption and fluorescence spectra of CP47 at 4 K, in an attempt to probe the electronic structure of bound chlorophylls. They focused their attention on the lowest energy electronic transition of chlorophyll *a*, the Q_y(0–0) transition around 675 nm. The linear dichroism and anisotropy spectra provided evidence that the Q_y(0–0) absorption envelope is composed of bands at 660, 668, 677, and 691 nm. It is not clear if any or all of these bands arise from different populations of monomeric chlorophylls or from excitonic interactions among closely spaced chlorophylls. If excitonic interactions are important, then they must be weak, on the order of 680 cm^{-1}, which represents the energy gap between 660 and 691 nm. Weak excitonic coupling appears to be characteristic of almost all chlorophyll *a*-binding proteins and represents an important contrast to the large excitonic splittings observed in the reaction centers and antennas of purple and green bacteria (Hawthornthwaite & Cogdell, 1991).

The studies of van Dorssen et al. (1987) contribute significantly to our understanding of energy transfer in CP47. However, electronic absorption and emission studies of protein-bound chromophores are not capable of providing a satisfactory level of structural and functional detail. For example, deconvolution of the Q_y(0–0) envelope does not give insight into specific interchromophore or chromophore–protein interactions that may be important determinants of function. Furthermore, absorption spectroscopy alone cannot determine functional heterogeneity in a sample of CP47; i.e., do all of the observed bands correspond to functional chlorophylls? Such information may be obtained with techniques with intrinsically higher resolution, such as infrared or Raman spectroscopies. Also, spectroscopic data of CP47 must be considered in conjunction with results from studies that address directly the kinetics of chlorophyll fluorescence within the protein.

In this paper, we report the structural and functional characterization of CP47 by spectroscopic techniques. Our main goal is to determine reliable means to distinguish between functional and nonfunctional centers in CP47 preparations. We have worked exclusively with samples that were prepared by solubilization with dodecyl β-maltoside and $LiClO_4$. It has been reported that PSII cores and CP47 isolated by this procedure (Ghanotakis et al., 1989) have a higher chlorophyll content (Dekker et al., 1989) and are more stable toward light (Ghanotakis et al., 1989) than samples that have been exposed to Triton X-100.

Time-resolved fluorescence measurements of CP47 and PSII core/CP47 complexes indicate that three lifetimes in the 0.05–3-ns range are associated with chlorophyll *a* molecules bound to CP47. A fourth lifetime around 6 ns is ascribed to fluorescence by inactive centers. In PSII core/CP47 complexes, a fifth lifetime is associated with recombination of the $P680^+Pheo^-$ state. Resonance Raman data on CP47 show that there are at least four structurally distinct populations of chlorophyll *a* in samples of CP47, each one exhibiting a characteristic vibrational frequency for the keto group of ring V ($\nu_{C=O}$). By evaluating Raman data at different excitation wavelengths, we were able to assign the $\nu_{C=O}$ vibrations to active and uncoupled chlorophyll *a*. Of the functional chlorophyll populations, at least one of the $\nu_{C=O}$ values

observed in CP47 is consistent with a hydrogen bond interaction between chlorophyll *a* and the protein. We suggest that this interaction results in significant modulation of the energies of the excited states of chlorophyll *a* molecules in that population. Hence, we conclude that interactions with the protein may play as important a role in determining the function of chlorophyll *a* in energy transfer as weak excitonic interactions.

MATERIALS AND METHODS

Sample Preparation. PSII core complexes and CP47 were prepared from spinach thylakoids as described by Ghanotakis et al. (1989). Complexes of the core plus CP47 were isolated according to Dekker et al. (1989). Prior to storage at −70 °C, samples were suspended in a buffer containing 20 mM 2-(*N*-morpholino)ethanesulfonic acid (Mes)/NaOH (pH 6.0), 0.4 M surose, 15 mM NaCl, 5 mM $MgCl_2$, 1 mM ethylenediaminetetraacetic acid (EDTA), and 0.014–0.030% dodecyl β-D-maltoside.

Samples for fluorescence spectroscopy were of concentrations of less than 10 μg of Chl/mL. Samples for Raman spectroscopy were of concentrations ranging from 0.33 to 1.83 mg of Chl/mL. All samples were prepared by suspension in the storage buffer described above, followed by stepwise addition, under nitrogen or argon, of 0.039 mg/mL catalase, 0.1 mg/mL glucose oxidase, and 20 mM glucose. This procedure scavenged most of the oxygen gas dissolved in the sample. Oxygen gas contributes to photodegradation of the sample, through a photodynamic effect mediated by chlorophyll excited states (Durrant et al., 1990).

We assessed the integrity of our samples by absorption spectroscopy, both before and after exposure to laser radiation. The method relies on the observation that binding of chlorophyll *a* to photosynthetic proteins induces a red shift in the high-wavelength bands [the so-called Q_y(0–0) transitions] of the chromophore, relative to the spectra observed in most polar and nonpolar solvents. Therefore, if our sample were to degrade by releasing chlorophyll from the protein and into the buffer, then we would have observed noticeable blue shifts in the absorption spectrum of protein-bound chlorophyll after exposure to the laser (Crystall et al., 1989; Booth et al., 1991). In all experiments reported in this paper, we did not observe shifts in the 675-nm band [Q_y(0–0) transition] of CP47 after acquisition of fluorescence data at continuous laser powers of 0.42–1.2 mW (1–3 nJ/pulse or 100–300 W peak power) for about 10 min at 10 °C. Similar analyses were conducted in PSII core and PSII core/CP47 complexes. Furthermore, no shifts in the absorption spectrum of CP47 were observed after acquisition of Raman data at continuous laser powers of 25–45 mW for up to 2 h at −90 °C. This indicates that our samples are not altered during exposure to laser radiation.

Fluorescence Lifetime Measurements. The kinetics of fluorescence decay of chlorophyll *a* were determined by the time-correlated single photon counting technique. The system housed at the NIH Regional Laser and Biotechnology Laboratories has been described in detail elsewhere (Holtom, 1990). Briefly, the laser system consisted of a Coherent Antares mode-locked Nd–YAG laser synchronously pumping a home-built single-jet, cavity dumped dye laser, operating at 3.8 MHz. Excitation at 620 nm (0.4–1.2 mW) was provided by pumping ethylene glycol solutions of rhodamine 6G or DCM. Fluorescence at 90° relative to excitation was collected at the magic angle, dispersed by a double monochromator in subtractive dispersive mode, and detected at 685 nm. The spectral band width for our measurements varied from 5 to 20 nm. These conditions optimize the detection of fluorescence from 685 to 695 nm (van Dorssen et al., 1987). The detector was a Hamamatsu R2809u-07 6-μm microchannel-plate photomultiplier tube. The electronics used for time-correlated single photon counting are described elsewhere (Holtom, 1990).

All samples treated in the manner described above were transferred to a quartz fluorescence cuvette (0.3 cm path length) and sealed. We obtained data at 10 °C over several time scales. Fast events under 1 ns were monitored by setting the multichannel analyzer to 3.8 ps/channel, yielding a full scale of 4 ns (1024 data points). Analysis of the excitation pulse under these conditions revealed the instrument response of our system, which was typically between 27 and 34 ps (full width at half-maximum). Data over 25- and 100-ns full scales were obtained with settings of 50.6 and 197–199 ps/channel, respectively (512 data points).

Analysis of Fluorescence Decay Data. We analyzed our fluorescence decay data by nonlinear least-squares fits of individual decay curves with the program LIFETIME (Holtom, 1990). Each decay curve was assumed to be composed of a sum of exponentials:

$$I(t) = \sum_i \alpha_i e^{-t/\tau_i} \tag{1}$$

where α_i and τ_i are the amplitude and lifetime of the *i*th decay component, respectively. From these data, the fluorescence yield of a component (Y_i) and mean fluorescence lifetime of a sample were given by

$$Y_i = \frac{\alpha_i \tau_i}{\sum_i \alpha_i \tau_i} \tag{2}$$

$$\tau_{mean} = \frac{\sum_i \alpha_i \tau_i^2}{\sum_i \alpha_i \tau_i} \tag{3}$$

LIFETIME convolutes the instrument response curve into the sample decay data and then performs a fit. The quality of the fits was assessed by a random distribution of residuals, a random distribution of the autocorrelation function (which should be distributed around zero, except for the first data point, where the autocorrelation value must be 1.0 for a good fit), and a value of the reduced χ^2 around 1.02. We have been particularly careful to avoid overfitting of our data, i.e., using more decay components than are *necessary and sufficient* to describe the data over a given time range. We present our fit results either as a decay curve with a superimposed fit and a plot of residuals (see Figure 1, for example) or simply as a plot of residuals (see Figure 2, for example). The latter format is more compact and allows for better visualization of any problems associated with the fit. We report fluorescence lifetimes and amplitudes as averages (with standard deviations) of different fits performed on samples of a given protein complex. Therefore, data presented in Figures 1–5 are representative of one sample under a given set of excitation and emission conditions. The averages and standard deviations presented in Table 1 and 3 reflect the uncertainties associated with measurements with different samples, with slight variations in laser power and stability from day to day, with slightly different detector settings, etc.

Resonance Raman Spectroscopy. Raman spectroscopy was carried out at Haverford College with an apparatus described

previously (de Paula et al., 1992). Briefly, excitation at 441.6 nm (25–45 mW) was provided by a Liconix 2040N He–Cd laser. Samples were held in 4-mm o.d. quartz tubes, which were then placed in a Wilmad 708–SJH cryostat. The temperature inside the cryostat was varied by flowing cold nitrogen gas through it. Typically, our measurements were conducted between −100 and −40 °C. During illumination by the laser, the sample was spun to minimize local heating and photodegradation.

The laser beam was focused with either a cylindrical or a spherical lens, with the focal plane of the lens placed about 5–10 mm in front of the quartz sample tube. Radiation was collected in the backscattering geometry. The excitation wavelength was filtered by an Omega Filters sharp edge filter (75% transmittance at 449 nm) and the remaining scattered light was focused into the entrance slit of an ISA THR-1000 1.0-m spectrograph. A 1800 groove/mm holographic grating dispersed the Raman scattered light, which was analyzed by a microcomputer-controlled Princeton Instruments IRY-1024/B diode array detector.

Data were collected with a spectral resolution of 6–8 cm^{-1}. A spectrum of the buffer solution was subtracted digitally from the spectrum of the solution containing the 47-kDa protein. Only such background-corrected spectra are presented in this paper. The spectra were calibrated with the Raman spectrum of a standard solution that was 2:1 acetone: *p*-methoxytoluene (spectrophotometric grade, Aldrich, Milwaukee, WI). This sample provided useful calibration bands at 1712, 1616, 1593, 1381, and 1291 cm^{-1}.

Analysis of Raman Data. Fitting of Raman spectra were performed with the program PEAKFIT 3.0 (Jandel Scientific, San Rafael, CA). Complex regions of the spectrum were assumed to be composed of a mixture of bands with Gaussian line shapes:

$$I = \frac{I}{\Gamma_D}\left(\frac{\ln 2}{\pi}\right)^{1/2} \exp\left[\frac{-\ln 2(\nu - \nu_0)^2}{\Gamma_D^2}\right] \qquad (4)$$

where ν is the vibrational frequency, ν_0 is the center frequency for the band, and Γ_D is a half-width parameter. PEAKFIT uses the Levenberg–Marquardt algorithm for nonlinear least-squares fitting of the data. Each Gaussian band is characterized by three parameters: amplitude, frequency, and width. In addition, each calculation included a fit of the baseline to a cubic polynomial. The quality of a given fit was assessed by a random distribution of residuals, a correlation coefficient (r^2) close to 1.00, and low values for the sum of the squares (X^2) and for the fit standard error.

RESULTS

Chlorophyll Fluorescence Decay Kinetics of CP47. Figures 1 and 2 show fits to the chlorophyll fluorescence decay kinetics of CP47 solubilized in 0.03% dodecyl maltoside (pH 6.0, 10 °C). Fits over a 25-ns time window (50.6 ps/channel) show that four exponentials are necessary to describe the data accurately (Figure 1) with $\chi^2 = 1.074$. Removal of a ~160-ps phase degrades the fit, giving $\chi^2 = 1.094$. The components with lifetimes < 1 ns were determined more accurately by performing measurements at 3.8 ps/channel (Figure 2). In this time window, three exponentials are necessary to fit the data (Figure 2a). Removal of the shortest component increases χ^2 and causes the residuals to become nonrandom early in the decay (Figure 2b). We summarize our results in Table 1. Fits of data over a 25-ns window were used to determine the 3.22- and 5.41-ns lifetimes. Fits over 4 ns were used to describe accurately the 75.8-ps and 1.05-ns lifetimes.

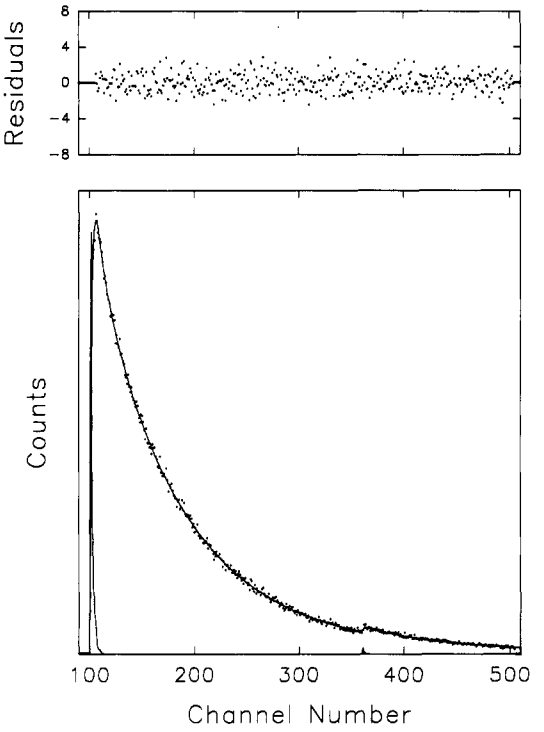

FIGURE 1: Chlorophyll fluorescence decay kinetics in the 47-kDa antenna protein (CP47) of spinach PSII (pH 6.0, 10 °C). Emission was observed at 685 nm; the multichannel analyzer was set at 50.6 ps/channel (512 channels); other experimental conditions are explained in the text. Bottom: experimental fluorescence decay curve (dots), the best fit to the data (solid line), and the instrument response (sharp trace). Top: plot of residuals for a four-exponential fit to the data. Fit parameters (numbers in parentheses are relative amplitudes): $\tau_1 = 0.166$ ns (13%); $\tau_2 = 0.655$ ns (10%); $\tau_3 = 3.38$ ns (47%); $\tau_4 = 5.56$ ns (30%); $\chi^2 = 1.074$.

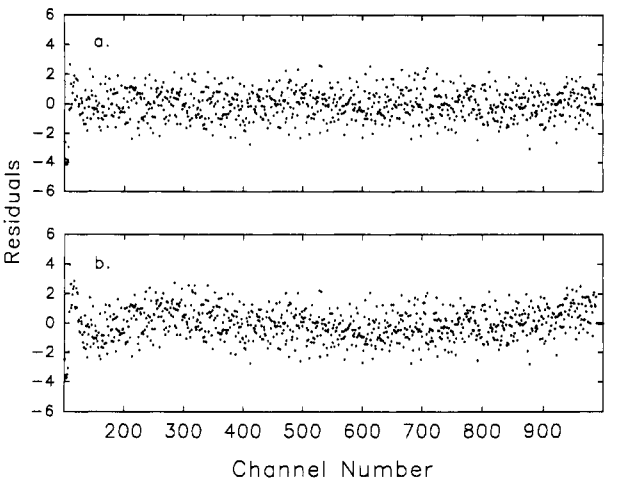

FIGURE 2: Chlorophyll fluorescence decay kinetics in CP47 (pH 6.0, 10 °C). Emission was observed at 685 nm; the multichannel analyzer was set at 3.8 ps/channel (1024 channels); other experimental conditions are explained in the text. (a) Plot of residuals for a three-exponential fit to the data. Fit parameters: $\tau_1 = 0.0886$ ns (19%); $\tau_2 = 1.53$ ns (33%); $\tau_3 = 5.57$ ns (49%); $\chi^2 = 1.076$. (b) Plot of residuals for a two-exponential fit to the data. Fit parameters (numbers in parentheses represent relative amplitudes): $\tau_1 = 0.184$ ns (21%); $\tau_2 = 3.54$ ns (79%); $\chi^2 = 1.248$.

At about 10 °C, the sign and magnitude of the amplitudes of these four decay components showed no significant dependence on the spectral band width of the emission monochromator, which ranged from 5 to 20 nm. The uncertainties in α are related more strongly to other experimental paameters, such as variations from sample to sample. Because we observed only positive values of α at 10 °C, we

Table 1: Summary of Chlorophyll Fluorescence Decay Data for CP47, the PSII Core, and the PSII Core/CP47 Complex[a]

sample	τ_i (ns)
CP47	0.0758 ± 0.0164
	1.05 ± 0.42
	3.22 ± 0.23
	5.41 ± 0.21
PSII core	0.054 ± 0.007
	0.45 ± 0.15
	3.54 ± 0.24
	6.48 ± 0.03
	29.04 ± 0.09
PSII core/CP47	0.0705 ± 0.0035
	0.468 ± 0.009
	3.11 ± 0.71
	7.06 ± 0.02
	26.83 ± 0.14

[a] Conditions: 0.03% dodecyl β-maltoside, pH 6.0. The τ values are averages of values obtained by fits of individual decay curves with the LIFETIME package (see the Materials and Methods section for details).

Table 2: Summary of Chlorophyll Fluorescence Decay Data Used in the Calculation of Average Fluorescence Lifetimes[a]

sample	α_i (arbitrary units)	τ_i (ns)	τ_{mean} (ns)
CP47[b]	0.084	0.120	2.93
	0.016	0.523	
	0.053	3.22	
PSII core[c]	0.097	0.279	12.99
	0.078	3.03	
	0.006	29.0	
PSII core/CP47[c]	0.448	0.448	8.89
	0.242	2.80	
	0.011	26.8	

[a] Conditions: 0.03% dodecyl β-maltoside, pH 6.0. The α and τ values are averages of values obtained by fits of individual decay curves with the LIFETIME package (see the Materials and Methods section for details.) The amplitude values are taken directly from the programs's output and have not been normalized. The component due to uncoupled chlorophylls (see text) was not used in the calculation of τ_{mean} (eq 3). [b] Average values of α and τ are from data obtained with a 25-ns time window (representative data are displayed in Figure 1). [c] Average values of α and τ are from data obtained with a 100-ns time window (representative data are displayed in Figure 4).

cannot assign directly any of these components to energy transfer processes. It is possible that direct evidence for energy transfer in CP47, vis-a-vis a combination of fluorescence rises and decays with specific spectral characteristics, can be obtained at lower temperatures. This was shown recently for the decay-associated spectra of the PSII core (Roelofs et al., 1991), where only at 77 K were fluorescence rises detected unambiguously. We are in the process of carrying out similar experiments on CP47.

The magnitudes of the four lifetimes allow us to provide a model for the function of chlorophyll *a* in CP47. The longest lifetime, $\tau = 5.41$ ns, correlates well with fluorescence lifetimes for chlorophyll *a* in organic solvents and detergents. For example, Connolly et al. (1982) report fluorescence lifetimes of 6.44, 6.09, 6.05, and 5.44 ns for chlorophyll *a* dissolved in pyridine, ether, toluene, and methanol, respectively. Also, Brown et al. (1983) measured a fluorescence lifetime of 5.8 ns for chlorophyll *a* dissolved in aqueous Triton X-100. In light of this correlation, we conclude that the 5.41-ns phase arises from chlorophyll *a* molecules bound to centers that are inactive in energy transfer or from monomeric chlorophyll *a* molecules that have been removed from the protein and are embedded in detergent micelles.

The remaining three components described in Table 1 have $\tau < 5$ ns. From the discussion above, it follows that these lifetimes are consistent with emission that is quenched, probably by energy transfer. The decay times and amplitudes of these short components were used to calculate the average fluorescence lifetime of CP47, according to eq 3 (Table 2). Thus traces with full scales of 25 ns were used to extract the α_i and τ_i values of all components, except the 5.41-ns component, which does not correspond to quenched chlorophyll emission. The τ_{mean} value of 2.93 ns is large because the fluorescence of CP47 is dominated by components with $\tau >$ 1 ns. On the average, the 75.8-ps component contributes only 14% to the decay, whereas the ~1- and ~3-ns components together contribute 64% to the fluorescence. Typically, the uncoupled chlorophyll emission is responsible for 22% of the total fluorescence intensity.

We set out to determine whether the short-lifetime components ($\tau < 5$ ns) described in Table 1 arise exclusively from intact centers, i.e., those centers that are capable of energy transfer to the PSII core. To this end, we assessed the effect of binding of CP47 to the PSII core on the fluorescence decay kinetics. We also examined the fluorescence decay kinetics of PSII core/CP47 complexes treated with Triton X-100, in order to determine the behavior expected of a sample that is impaired in energy and electron transfer. These experiments are described below.

Chlorophyll Fluorescence Decay Kinetics of the PSII Core Solubilized in Dodecyl β-Maltoside. Table 1 summarizes the chlorophyll fluorescence decay kinetics in the PSII core at 685 nm. Our data are in qualitative agreement with those of Roelofs et al. (1991), who observed decay components with $\tau = 41$ ps, 0.16 ns, 1.09 ns, 5.87 ns, and 29.6 ns in PSII cores solubilized in Triton X-100. Roelofs et al. (1991) also extracted a 2-ps component from their decay traces. This 2-ps component may be related to the formation of $P680^+Pheo^-$ (Wasielewski et al., 1989a,b; Roelofs et al., 1991). Our least-squares fitting package did not provide evidence that more than five exponentials were necessary and sufficient to describe our data on PSII cores out to 100 ns full scale. However, we do not discount the existence of a 2-ps component because ultrafast electron transfer is indeed a mechanism by which fluorescence may be quenched.

The 41-ps, 5.9-ns, and 30-ns components observed by Roelofs et al. (1991) in PSII cores are analogous to the 54-ps, 6.5-ns, and 29.0-ns components we observe in our samples (Table 1). The 0.16- and 1.1-ns components observed by Roelofs et al. (1991) correlate only weakly with the 0.45-ps and 3.54-ns components of our fits. As will be shown later, the presence of a ~1-ns decay component may suggest damaged centers in the sample. Therefore, we ascribe differences in the intermediate decay components to the use of Triton X-100 by Roelofs et al. (1991) in their isolation of the cores.

In spite of some differences between our data and those of Roelofs et al. (1991), it is possible to use their data and those of other investigators to propose assignments for the five decay components that we observe in PSII cores solubilized with dodecyl β-maltoside. These assignments will help the interpretation of the data on PSII core/CP47 complexes.

According to fluorescence decay studies carried out at 77 K by Roelofs et al. (1991), the decay component with $\tau =$ 40–50 ps is a result of energy transfer between chlorophyll species emitting at 672 and 683 nm. The latter is probably P680.

The 29-ns lifetime corresponds to charge recombination from the $P680^+Pheo^-$ state (Mimuro et al., 1988; Govindjee et al., 1990; Booth et al., 1991; Roelofs, et al., 1991). The intermediate component at 6.48 ns correlates well with the fluorescence lifetime of chlorophyll *a* dissolved in organic

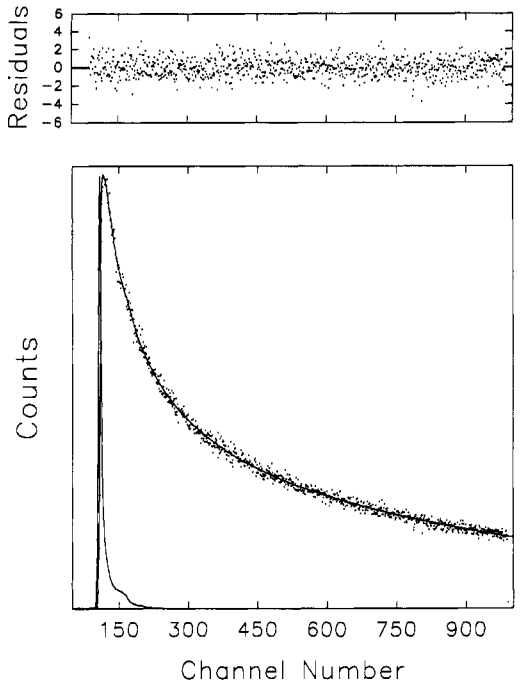

FIGURE 3: Chlorophyll fluorescence decay kinetics in the PSII core/CP47 complex (pH 6.0, 10 °C). Emission was observed at 685 nm; the multichannel analyzer was set at 3.8 ps/channel (1024 channels); other experimental conditions are explained in the text. Bottom: experimental fluorescence decay curve (dots), the best fit to the data (solid line), and the instrument response (sharp trace). Top: plot of residuals for a three-exponential fit to the data. Fit parameters (numbers in parentheses are relative amplitudes): τ_1 = 0.0729 ns (53%); τ_2 = 0.475 ns (21%); τ_3 = 3.49 ns (26%); χ^2 = 0.962.

solvents (*vide supra*). We assign this component to monomeric chlorophyll *a* in solution or bound to completely denatured centers.

Components with lifetimes around 0.45 and 3.5 ns have been observed by several groups (Roelofs et al., 1991; Govindjee et al., 1990, Booth et al., 1990) but definitive assignments have not been made. Our own data on PSII cores and PSII core/CP47 complexes, presented below, provide insight into the origins of these components.

Chlorophyll Fluorescence Decay Kinetics of the PSII Core/CP47 Complex Solubilized in Dodecyl β-Maltoside. Chlorophyll fluorescence decay kinetics at 685 nm for the PSII core/CP47 complex are shown in Figures 3 and 4, and the results are summarized in Tables 1 and 2. Binding of CP47 to the PSII core lowers the average fluorescence lifetime of the core by 32% (Table 2). Most of the short-lifetime components (<7 ns) are shorter in the PSII core than in the PSII core/CP47 complex. However, both the lifetime and the amplitude of the charge recombination component (τ = 27–29 ns) component decrease significantly in the PSII core/CP47 complex, in relation to the PSII core. Hence, the reduction in τ_{mean} must be due to changes in the yield of the charge recombination component.

There is close correspondence between the emission patterns of the PSII core and the PSII core/CP47 complex: both samples exhibit five lifetimes of similar (but not identical) magnitudes. Consequently, our conclusions for the PSII core may be used to interpret the data on the PSII core/CP47 complex.

Three of the decay components of the PSII core/CP47 complex may be assigned by inspection of the data in Table 1. First, the 27-ns component is due to charge recombination in centers that stabilize the $P680^+Pheo^-$ state effectively.

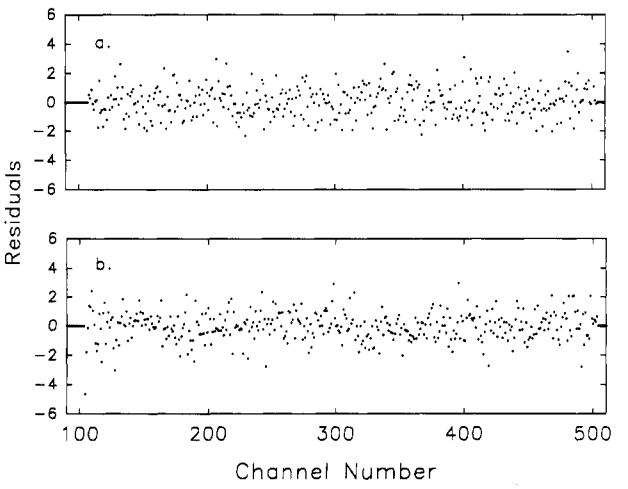

FIGURE 4: Chlorophyll fluorescence decay kinetics in the PSII core/CP47 complex (pH 6.0, 10 °C). Emission was observed at 685 nm; other experimental conditions are explained in the text. (a) Plot of residuals for a four-exponential fit to data obtained at 50.6 ps/channel (512 channels). Fit parameters (numbers in parentheses represent relative amplitudes): τ_1 = 0.1066 ns (58%); τ_2 = 0.826 ns (12%); τ_3 = 3.61 ns (22%); τ_4 = 10.08 ns (8%); χ^2 = 1.097. (b) Plot of residuals for a four-exponential fit to data obtained at 196.6 ps/channel (512 channels). Fit parameters: τ_1 = 0.265 ns (53%); τ_2 = 2.80 ns (28%); τ_3 = 7.06 ns (17%); τ_4 = 26.7 ns (1%); χ^2 = 1.001.

Second, the 7-ns component is due to uncoupled monomeric chlorophyll *a*. Third, the 70.5-ps component may be assigned to efficient energy transfer, although it is not certain if the events leading to this lifetime are localized onto CP47 or the reaction center or reflect interactions between the antenna and the reaction center.

The 0.47- and 3.11-ns components must be analyzed with more care, because both the reaction center core and CP47 exhibit decay components in the 0.4–3-ns range. In order to help identify these components as arising from functional and nonfunctional centers, we performed experiments under slightly denaturing conditions, as shown below.

Chlorophyll Fluorescence Decay Kinetics of the PSII Core/CP47 Complex Treated with Triton X-100. Exposure of stable PSII core samples to the detergent Triton X-100 not only destabilizes the reaction center toward exposure to light (Akabori et al., 1988) but also releases chlorophylls from the reaction center (Dekker et al., 1989). We determined the fluorescence decay kinetics in PSII cores and in PSII core/CP47 complexes that were prepared by solubilization in dodecyl maltoside but then were diluted (under an argon atmosphere) in a buffer containing 0.2% (w/v) Triton X-100 and the O_2-scavenging system (see Materials and Methods). The data are shown in Figure 5 and summarized in Table 3.

We observe that exposure to Triton X-100 results in the disappearance of the 50–70-ps component. While a 0.7–1.0-ns component remains, a ~6-ns component dominates the decay (94–97%). Four important conclusions may be drawn from these experiments:

(i) Treatment of PSII core preparations with Triton X-100 suppresses energy transfer events in both the D1/D2 core and in CP47, as evidenced by the disappearance of the 50–70-ps components.

(ii) A ~3-ns component is not observed in Triton-treated samples. This suggests that lifetimes in this range are associated with intact or near-intact centers in the samples described in Table 1. Namely, the 3.22-ns component of CP47 may be assigned to functional chlorophyll. Likewise, the 3.54-ns component of the PSII core may be assigned to a process that is very sensitive to interchromophoric interactions.

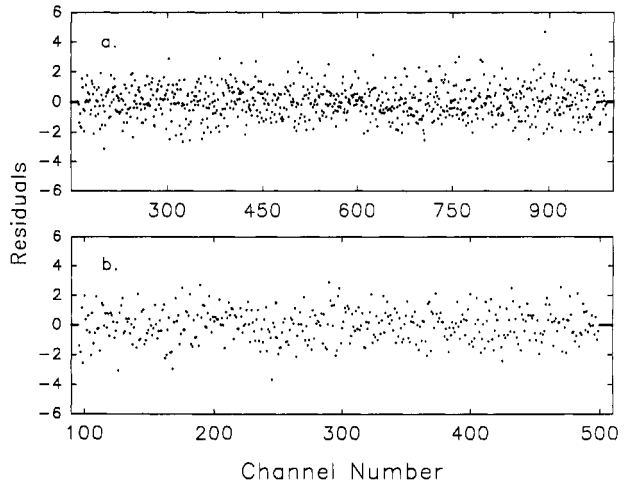

FIGURE 5: Chlorophyll fluorescence decay kinetics in samples treated with 0.2% Triton X-100, as described in the text (pH 6.0, 10 °C). Emission was observed at 685 nm; other experimental conditions are explained in the text. (a) PSII core. Plot of residuals for a two-exponential fit to data obtained at 9.6 ps/channel (1024 channels). Fit parameters (number in parentheses represent relative amplitudes): $\tau_1 = 0.69$ ns (5%); $\tau_2 = 5.68$ ns (95%); $\chi^2 = 1.078$. (b) PSII core/CP47 complex. Plot of residuals for a two-exponential fit to data obtained at 20.4 ps/channel (512 channels). Fit parameters: $\tau_1 = 1.23$ ns (3%); $\tau_2 = 5.91$ ns (97%); $\chi^2 = 1.144$.

Table 3: Summary of Chlorophyll Fluorescence Decay Data for the PSII Core and the PSII Core/CP47 Complex Treated with 0.2% Triton X-100 (pH 6.0)

sample	τ_i (ns)
PSII core	0.702 ± 0.223
	5.82 ± 0.24
PSII core/CP47	1.02 ± 0.30
	5.92 ± 0.02

(iii) Denatured centers exhibit components with subnanosecond lifetimes. It is possible that the process giving rise to these lifetimes is inefficient energy transfer in centers that are perturbed structurally. The results indicate that the 1.05-ns component of CP47 may arise from such perturbed centers. Likewise, it is possible that components in the 0.4–1.0-ns range, observed by many groups in PSII cores [Table 1; also Roelofs et al. (1991), Booth et al. (1991), and Govindjee et al. (1990)], are due to energy transfer in perturbed reaction centers.

(iv) Although it is possible to assign the 3.22-ns component of CP47 to functional chlorophyll, we cannot ascertain from the data sunmmarized in Tables 1 and 3 if fluorescence from this component is quenched upon binding to the PSII core. This is because the 3.11-ns component of the PSII core/CP47 complex may be a composite of an unquenched 3.2-ns component of CP47 and the 3.5-ns component of the reaction center.

Resonance Raman Spectroscopy of CP47. Of the proteins investigated above by fluorescence techniques, the PSII core has been characterized by resonance Raman spectroscopy (Ghanotakis et al., 1989; Möenne-Loccoz et al., 1989; de Paula et al., 1990). Although vibrational spectroscopy of the PSII core/CP47 complex has the potential to answer important questions concerning structure and function, the vast number of bound and uncoupled pigments in different sites (chlorophylls and carotenes in CP47 and the core; pheophytins in the core only) would make analysis of the spectrum difficult. On the other hand, analysis of the vibrational spectrum of chlorophyll *a* in CP47 should be possible. Such studies provide an important link to the fluorescence data discussed above.

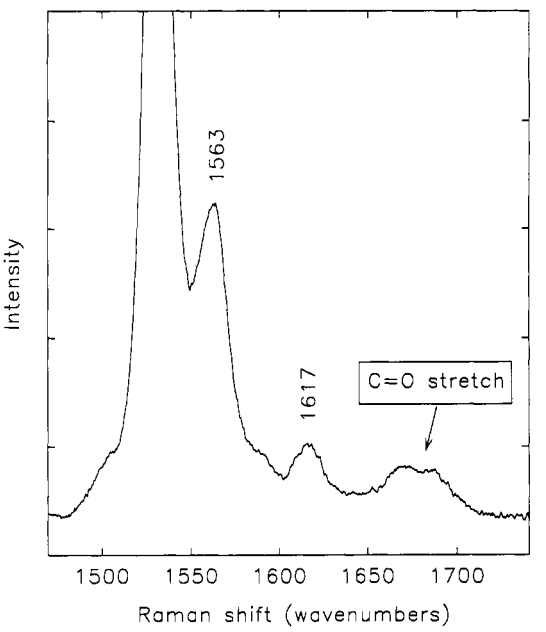

FIGURE 6: High-frequency region of the resonance Raman spectrum of CP47 with excitation at 441.6 nm (pH 6.0, −90 °C). All other experimental conditions were as in the text.

We obtained resonance Raman spectra of CP47 in an attempt to determine whether there are structural features that provide further insight into the heterogeneity observed via kinetic methods. This vibrational technique has been used successfully in the study of chlorophyll-binding proteins because of its sensitivity toward specific interactions between chromophores or between chromophore and the surrounding protein [reviewed by Lutz and Mäntele (1991) and Lutz and Robert (1988)].

Figure 6 shows the high-frequency region of the resonance Raman spectrum of CP47, obtained with excitation at 441.6 nm. This laser wavelength is nearly coincident with the Soret absorption maximum for chlorophyll *a* bound to CP47, 439 nm (Ghanotakis et al., 1989). The main features of the Soret-excited spectrum have been discussed previously (de Paula et al., 1990). Briefly, the band at 1530 cm^{-1} is due to a C–C stretch of *all-trans*-β-carotene, another light-harvesting pigment bound to CP47. This band is observed with excitation at 441.6 nm because at this wavelength there is residual oscillator strength from the β-carotene electronic transition centered at 490 nm. Based on resonance Raman and infrared measurements of chlorophyll *a* in solution (Fujiwara & Tasumi, 1986), we assign the bands at 1563 and 1617 cm^{-1} to C–C stretches of five-coordinate chlorophyll *a*. The lack of fine structure in these bands indicates that all chlorophylls bound to CP47 assume a coordination number of five. The broad feature centered at roughly 1690 cm^{-1} is due to a C–O stretch from the C_9 keto group of chlorophyll *a* (Figure 7). No other vibrational modes from either chlorophyll or β-carotene appear in this region of the spectrum (Lutz and Mäntele, 1991; Lutz and Robert, 1988; Tasumi and Fujiwara, 1987).

It is clear that the carbonyl stretching region of the Raman spectrum in Figure 6 is complex, showing at least two peaks and a long tail to higher frequencies. As only one carbonyl group of each chlorophyll *a* is active in its resonance Raman spectrum (the ester groups emanating from positions 7 and 10 are not conjugated with the ring), our data suggest that there are at least two populations of chlorophyll *a* bound to CP47. In order to clarify this point, we attempted a deconvolution

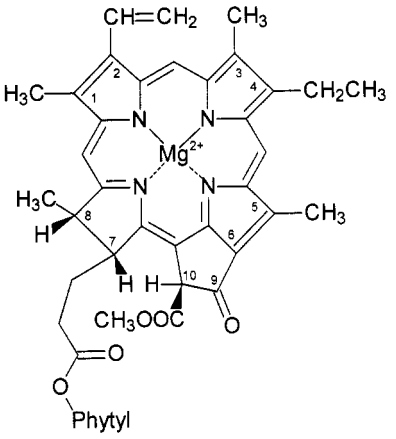

FIGURE 7: Structure of chlorophyll *a*, showing the Fisher numbering system used in the text.

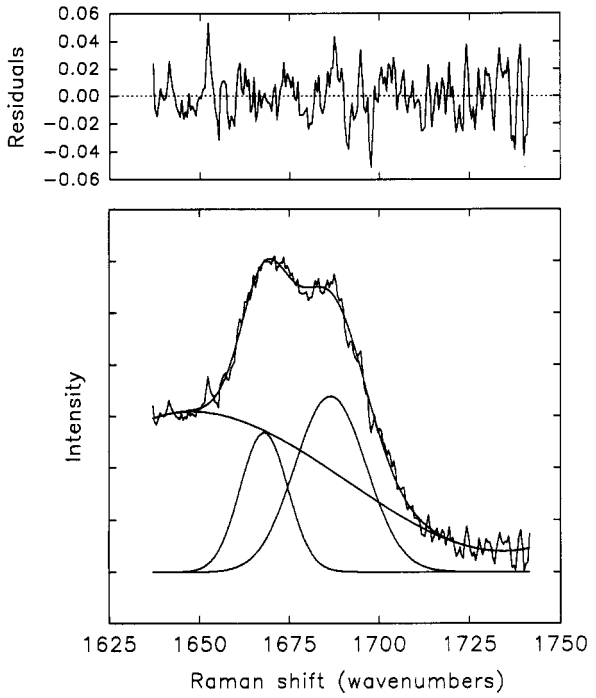

FIGURE 8: Carbonyl stretching region of the resonance Raman spectrum of the 47-kDa protein. The lower box contains the observed spectrum, the spectrum calculated from the mixture of two Gaussian bands, the individual Gaussian bands, and the calculated baseline. The upper box shows the plot of relative residuals for the fit. Fit parameters: band 1 – ν = 1668 cm^{-1}, full width at half-maximum (FWHM) = 16 cm^{-1}, amplitude = 0.268; band 2 – ν = 1686 cm^{-1}, FWHM = 23 cm^{-1}, amplitude = 0.339; r^2 = 0.9926; X^2 = 0.0645; fit standard error = 0.01770.

of the resonance Raman spectrum of CP47 in the 1650–1750-cm^{-1} region. The results are shown in Figures 8 and 9.

A reasonably satisfactory fit may be accomplished with a mixture of two Gaussian bands centered at 1668 and 1686 cm^{-1} (Figure 8). However, in order to fit the high-frequency wing of the spectrum, a very large width must be ascribed to the 1686-cm^{-1} component (23 cm^{-1} at half-maximum). This sacrifices the fit in the region between the 1668- and 1686-cm^{-1} bands. The problem could be circumvented by increasing the width of the 1668-cm^{-1} component, but this action would affect adversely the fit of the low-frequency wing of the 1668-cm^{-1} component, which falls off sharply.

In light of the above, we are left with two possibilities for calculating the spectrum: (i) fitting to two asymmetric bands with sharp low-frequency sides and broad high-frequency sides, or (ii) inclusion of a third weak component to fit the broad

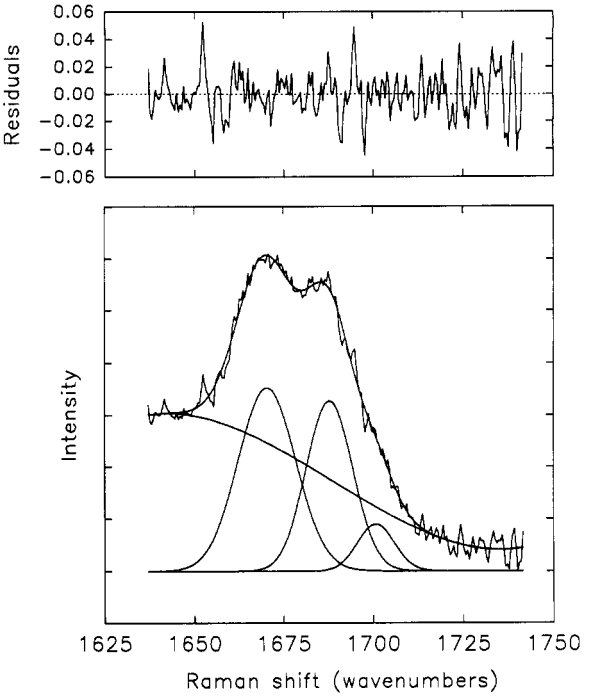

FIGURE 9: Carbonyl stretching region of the resonance Raman spectrum of the 47-kDa protein. The lower box contains the observed spectrum, the spectrum calculated from the mixture of three Gaussian bands, the individual Gaussian bands, and the calculated baseline. The upper box shows the plot of relative residuals for the fit. Fit parameters: band 1 – ν = 1670 cm^{-1}, full width at half-maximum (FWHM) = 19 cm^{-1}, amplitude = 0.353; band 2 – ν = 1688 cm^{-1}, FWHM = 15 cm^{-1}, amplitude = 0.328; band 3 – ν = 1701 cm^{-1}, FWHM = 12 cm^{-1}, amplitude = 0.0900; r^2 = 09933; X^2 = 0.0579; fit standard error = 0.01688.

high-frequency part of the spectrum. The first situation could arise from two continuous distributions of C=O frequencies in the sample: one with a maximum at 1668 cm^{-1} and another with a maximum at 1686 cm^{-1}. In order to explain the asymmetric line shapes, we must assume that the distributions are skewed to the high-frequency side, falling off sharply at frequencies below the peak maximum. This scenario is possible but is unusual. Mathematically, this would introduce a great number of parameters to the fit, so that a good fit would be almost guaranteed regardless of the physical relevance of the model. The second situation provides a simpler (although not simplistic) model of the data. Because we fit to Gaussians, inhomogeneity is also implied. However, fitting to three Gaussian bands assumes that there are three symmetrical distributions with three distinct medians and standard deviations. Mathematically, only nine parameters require adjustment, with at least four (the intensities and positions of the ~1670- and ~1685-cm^{-1} bands) being fairly rigid. Thus, statistical evaluation of goodness-of-fit is reliable and straightforward. For these reasons, we have chosen to proceed with a three-band fit of the C=O stretching region.

In Figure 9, a three-band fit of the spectrum is shown. Compared to the fit in Figure 8, introduction of a band at 1701 cm^{-1} improves the fit statistics, results in a better fit of the region between the 1688- and 1670-cm^{-1} components, and returns Gaussians with half-widths that are physically relevant (12–19 cm^{-1}). Addition of a fourth, very weak band to the fit at the low-frequency wing (1663 cm^{-1}) did not improve the fit considerably (r^2 = 0.9935; X^2 = 0.0560, data not shown). Therefore, a mixture of three Gaussian bands is both necessary and sufficient to fit the C=O region of the Raman spectrum of CP47.

We conclude from the analysis of data obtained with 441.6-nm excitation that there are more than two populations of chlorophylls *a* bound to CP47. Each population may be distinguished by a characteristic frequency for the C_9 keto group of chlorophyll *a*. No other high-frequency feature of the spectrum shows the heterogeneity apparent in the C=O stretching region.

We probed the C=O stretching region further by examining published resonance Raman spectra of CP47 at other excitation wavelengths. Previous work at 406.7 nm (de Paula et al., 1990) afforded a spectrum dominated by a strong feature at 1693 cm^{-1}, with a weak shoulder at 1669 cm^{-1}. The 1669-cm^{-1} band is likely to arise from the same electronic origin that resulted in a strong spectrum with 442-nm excitation—ostensibly the species giving rise to the 439-nm absorption band of the protein. Because of the differences in enhancement patterns, it is possible that the 1693-cm^{-1} band is distinct from those bands observed with excitation at 442 nm.

The excitation wavelength of 406.7 nm is some 32 nm to the blue of the Soret maximum and some 14 nm to the blue of the η-band maximum for the protein. By contrast, the Soret and η-band maxima of monomeric chlorophyll *a* in diethyl ether occur at 430 and 410 nm, respectively (Hoff & Amesz, 1991). Therefore, it is possible that excitation at 406.7 nm probes preferentially (although not exclusively) chlorophyll molecules with η-band maxima near this wavelength. Monomeric chlorophyll *a* is a particularly relevant example.

We suggest that the 1693-cm^{-1} band observed with 406.7-nm excitation (de Paula et al., 1990) arises from a unique population of chlorophyll *a* molecules in samples of CP47. We further assign this population to monomeric chlorophyll *a* in severely denatured centers. In support of this conclusion, we cite the following evidence:

(i) Monomeric chlorophyll species are present in the sample, as shown by the fluorescence decay data presented above.

(ii) According to extensive studies in solution, the 1693-cm^{-1} band is consistent with a $\nu_{C=O}$ band from monomeric, five- or six-coordinate chlorophyll *a* in aprotic solvents (Krawczyk, 1989).

(iii) The excitation wavelength of 406.7 nm is nearly coincident with the strong η band of monomeric chlorophyll *a* in a variety of solvents (Hoff & Amesz, 1991). In contrast, 406.7 nm is far removed from either the Soret or η-band maxima of the protein (439 and 421 nm, respectively).

(iv) Raman excitation profiles of the $\nu_{C=O}$ mode in a chlorophyll *a* dimer show only two sharp and strong maxima at the peaks of the Soret and η absorption bands (Thibodeau and Koningstein, 1989). The frequency of the C_9=O vibration does not change throughout the excitation profile. These observations suggest that η-band excitation provides a powerful probe of the C_9=O vibration. Also indicated is that a *strong* 1693 cm^{-1} band is not likely to arise from vibronic contributions of the *protein* Soret or η bands when the excitation is in resonance with the η-band of another species, such as monomeric chlorophyll in solution.

In summary, data obtained at two excitation wavelengths allow us to observe four populations of chlorophyll *a* bound to CP47, each with a distinctive $\nu_{C=O}$ vibration (Table 4). On the basis of the enhancement patterns, we associate the populations exhibiting $\nu_{C=O}$ = 1670, 1688, and 1701 cm^{-1} with protein-bound chlorophyll *a*. A population exhibiting $\nu_{C=O}$ = 1693 cm^{-1} arises from uncoupled chlorophyll *a*. Our strategy for assignment of the Raman spectrum of CP47 has precedent. De Paula et al. (1990) and Möenne-Loccoz et al. (1989) used a similar approach to assign the C=O stretching frequencies of chlorophylls ($\lambda_{max} \sim 436$ nm) and pheophytins ($\lambda_{max} \sim 416$ nm) bound to the PSII core.

Table 4: Summary of C_9 Keto Group Vibrations for Chlorophyll *a* Bound to CP47 (pH 6.0, −90 °C)

ν (cm^{-1})	assignment
1670	protein-bound chlorophyll *a*; C_9=O group is hydrogen-bonded; $\Delta\lambda_Q$ = 3.8 nm
1688	protein-bound chlorophyll *a*; C_9=O group is free of specific interactions with the medium
1693[a]	monomeric chlorophyll *a* in denatured centers or released from the protein; λ_Q = 660–665 nm
1701	protein-bound chlorophyll *a*; C_9=O group is free of specific interactions with the medium

[a] Obtained with 406.7-nm excitation (de Paula et al., 1990).

Like picosecond fluorescence, resonance Raman spectroscopy provides a level of structural and functional detail that is simply not available by steady-state absorption or fluorescence measurements (isotropic or anisotropic). When considered together, the static and time-resolved spectroscopic data allow us to assess the relationship between structure and function in the 47-kDa antenna protein of PSII. This is attempted below.

DISCUSSION

Energy and Electron Transfer in the PSII Core/CP47 Complex. Our results on PSII cores and PSII core/CP47 complexes show that partial denaturation with Triton X-100 removes components associated with fast energy transfer (50–70 ps) but retains a subnanosecond decay component (0.7–1.0 ns). Similar components have been observed in other PSII core preparations (Roelofs et al., 1991; Booth et al., 1991; Govindjee et al., 1990; this work) and in PSII core/CP47 complexes solubilized in dodecyl β-maltoside (Table 1). We propose that decay components in the 0.4–1.0-ns range are due to processes in structurally perturbed centers, where some, suboptimal interchromophoric communication still exists.

This process may be either fast charge recombination or slow energy transfer. Govindjee et al. (1990) have shown that the amplitude and lifetime of a decay component with τ = 0.32 ns in PSII cores do not change upon prereduction of the Pheo with sodium dithionite and methyl viologen in the dark. This result suggests that the 0.32-ns component does not arise from charge recombination. Therefore, we assign components in the 0.4–1.0-ns time scale to slow energy transfer in structurally perturbed PSII core and PSII core/CP47 centers.

Our fluorescence studies also indicate that a ~3.5-ns component is not observed in PSII cores and PSII core/CP47 complexes treated with Triton X-100. Some studies of the PSII core have assigned a ~4-ns decay component to a population of chlorophylls that is not connected to energy or electron transfer in the reaction center (Booth et al., 1991; Roelofs et al., 1991). This interpretation is challenged by Govindjee et al. (1990), who proposed that there is a continuous distribution of charge recombination times in the PSII core from 4 to 20 ns. The distribution of recombination rates is seen as evidence for a distribution of conformational substates in the reaction center. We provide below an alternative explanation that combines our own observations with those of Roelofs et al. (1991), Booth et al. (1991), and Govindjee et al. (1990).

Although we were not successful in fitting our data for the PSII core with Gaussian and Lorentzian distributions ($\chi^2 \gg 1.00$, data not shown), we cannot discount the results of Govindjee et al. (1990). These workers provided convincing evidence that connects the ~4-ns lifetime with charge recombination and performed measurements with a phase fluorometer, which is the equipment of choice for the determination of lifetime distributions (Alcala et al., 1987). Furthermore, our observation that a ~3.5-ns component is absent under denaturing conditions leads to the conclusion that the process associated with the ~3-ns decay is sensitive to pigment–pigment or pigment–protein interactions that are disrupted by Triton X-100. Electron transfer is clearly such a process. However, if the ~3-ns component is due to charge recombination in a percentage of the centers, then these centers must have structures that differ significantly from those of centers that stabilize the $P680^+Pheo^-$ state more effectively (τ = 29 ns). Hence, we agree with Govindjee et al. (1990) that structural heterogeneity gives rise to at least two charge recombination times: 3.5 and 29 ns in PSII cores and 3.1 and 27 ns in PSIi core/CP47 complexes. However, we postulate that the shorter charge recombination times are due to centers where structural factors that optimize charge separation are perturbed (e.g., donor–acceptor distance, vibronic coupling).

In summary, our fluorescence data indicate that samples of the PSII core and of the PSII core/CP47 complex are heterogeneous, with at least three classes of centers: (i) centers that are effective in energy transfer and stabilization of the $P680^+Pheo^-$ state (characterized by τ = 50–70 and 27–29 ns, respectively); (ii) centers with impaired function in energy transfer and stabilization of the $P680^+Pheo^-$ state (characterized by $\tau \sim 0.45$ and ~ 3 ns, respectively); and (iii) centers where chlorophyll–chlorophyll and chlorophyll–protein interactions have been disrupted completely ($\tau \sim 6$ ns).

Mechanism of Damage by Triton X-100. Our studies suggest further that the medium in which the PSII cores are solubilized contributes importantly to sample heterogeneity. Namely, Triton X-100 increases the proportion of centers with impaired function. The mechanism of damage to the PSII core by Triton X-100 has also been investigated by Tang et al. (1991). Their hole burning studies suggested that Triton X-100 disrupts energy transfer from an "accessory" chlorophyll to pheophytin. No evidence was seen for the release of pigments as a result of treatment with Triton X-100, an observation that prompted Tang et al. (1991) to propose that Triton X-100 merely perturbs the spatial relationships between pigments in the reaction center. Our results support the conclusion by Tang et al. (1991) that Triton X-100 affects energy transfer in the PSII core but also provide additional evidence that at least part of the effect is due to release of chlorophylls. This is because the fluorescence decay of Triton-treated samples is dominated by a ~6 ns component.

The persistence of a lifetime component at 0.7–1.0 ns in Triton-treated samples indicates that slow energy transfer is still occurring in some centers that have not lost pigments. These centers probably correlate with those damaged centers observed by Tang et al. (1991). Surely, our results correlate strongly with disruption of the process that results in the 50–70-ps component, i.e., energy transfer between a chlorin species that emits at 672 nm (Chl_{672}) and a species that emits at 683 nm (probably P680) (Roelofs et al., 1991). Also, energy transfer between CP47 and the PSII core is disrupted by treatment with Triton X-100.

In addition to describing the sources of heterogeneity of PSII core preparations, our experiments provide insight into the discrepancies in picosecond fluorescence data reported by different groups and discussed in the beginning of this paper.

It is clear that structural and functional heterogeneity may be found even in samples prepared with dodecyl β-maltoside only. However, our results indicate that Triton X-100 is capable of causing additional structural damage. As a consequence, it is reasonable that the use of Triton X-100 during any stage of the preparation of the PSII core may lead to large proportions of impaired centers.

Different research groups use slightly different stabilization protocols, which may vary in effectiveness. It is not surprising to see, therefore, a certain degree of variability in the fluorescence decay data for the PSII core. For example, the distribution of charge recombination lifetimes reported by Govindjee et al. (1990) may be a direct consequence of a structurally heterogenous sample produced by their stabilization protocol, which included precipitation of the reaction center with poly(ethylene glycol) and resuspension in 0.04% Triton X-100. Likewise, the appearance of a ~1-ns component in the data of Roelofs et al. (1991) may reflect a measurable proportion of perturbed centers in their samples, which were stabilized by resuspension in a buffer containing dodecyl β-maltoside. The differences in stabilization protocols and the structural heterogeneities caused by them may also help to explain reported discrepancies in the rates of primary charge separation in the PSII core (Wasielewski et al., 1989a; Hastings et al., 1992).

Assignment of the Fluorescence Lifetimes in CP47. The data presented above indicate that there is some heterogeneity in samples of CP47 solubilized in 0.03% dodecyl β-maltoside at pH 6.0. The 75.8-ps and 3.22-ns components of the fluorescence decay of CP47 may be associated with relatively intact centers. The 1.05-ns component probably arises from structurally perturbed centers, where some key interchromophoric interactions are disrupted. The 5.41-ns component arises from centers where all interchromophoric interactions have been disrupted.

The presence of perturbed centers with τ = 1.05 and 5.41 ns may be an inevitable result of the biochemical protocols that lead to the separation and purification of CP47. This is illustrated by the fact that none of the samples investigated for this report were devoid of perturbed centers, in spite of our use of mild separation conditions (Ghanotakis et al., 1989).

Our results indicate that the measurement of chlorophyll fluorescence decay kinetics with picosecond time resolution may represent one of the few viable assays for structural and functional integrity in CP47. Another assay method, reasonance Raman spectroscopy, is richer in structural detail and is discussed below.

Correlation between Emission Kinetics and Vibrational Properties in CP47. Our fluorescence decay and resonance Raman measurements are consistent with the presence of several populations of chlorophyll *a* bound to CP47 (Tables 1 and 3). Our measurements allow us to correlate the fluorescence lifetime and $\nu_{C=O}$ for only one of these populations, that arising from uncoupled chlorophylls. This population has τ = 5.41 ns and $\nu_{C=O}$ = 1693 cm^{-1}. Both parameters indicate that this population consists of monomeric chlorophylls, probably embedded in detergent micelles.

For the uncoupled chlorophylls of CP47 the Mg^{2+} ion is five-coordinate (de Paula et al., 1990) and the $C_9{=}O$ group does not appear to interact with the medium in a specific way, such as H-bonding (*vide infra*). Chlorophyll monomers with these structural features typically show Q_y(0–0) transitions in the 660–665-nm range (Krawczyk, 1989). Therefore, we

suggest that the population with $\nu_{C=O}$ = 1693 cm^{-1} corresponds to the 660-nm contribution to the linear dichroism spectrum of CP47, measured by van Dorssen et al. (1987).

The remaining populations of chlorophyll exhibit quenched emission–an indication of energy transfer within the protein. Our fluorescence measurements are not capable of detecting ultrafast equilibrium of excitation energy between chlorophyll populations that are closely spaced in the protein. Such processes are likely to occur within 3 ps, as has been demonstrated for the B800–B850 light-harvesting complex of *Rhodobacter sphaeroides* (Trautman et al., 1990). Furthermore, our results to date do not permit a direct correlation between the emission and vibrational properties of the populations bound to active CP47. Indeed, such strict correlations may not be obtainable, depending on the complexity of the mechanism of energy transfer and of excitonic interactions among the pigments. However, the relative importance of excitonic interactions and chromophore–protein interactions to the mechanism of energy transfer in CP47 can be addressed by scrutinization of the resonance Raman data, as shown below.

Correlation between Electronic and Vibrational Properties in CP47. The electronic structure of chlorophyll *a* bound to a protein may be affected by several factors. Excitonic interactions between closely spaced chromophores can be responsible for large shifts in the absorption bands of photosynthetic pigments. Such interchromophoric interactions are partly responsible for red-shifting the Q bands of bacteriochlorophylls in both light-harvesting and reaction center complexes from bacteria (Hawthorthwaite & Cogdell, 1991).

For monomeric or weakly-interacting chlorophylls, the immediate environment of the chromophore plays an important role in determining electronic structure. Extensive studies of chlorophyll *a* in solution have identified two factors that affect λ_Q, the wavelength of the lowest energy π–π^* electronic transition [Q_y(0–0) transition]: (i) The medium surrounding a chromophore affects the energies associated with electronic or vibrational transitions because the ground and excited states have different permanent dipole moments. As a consequence, the solvent may either stabilize or destabilize the excited state relative to the ground state. Krawczyk (1989) has shown that the solvent affects both λ_Q and $\nu_{C=O}$, the frequency of the C_9=O vibration of chlorophyll *a*. (ii) Hydrogen bonding between the solvent and the C_9=O group affects both $\nu_{C=O}$ and λ_Q because the C_9=O group is conjugated to the chlorin ring. Working with an extensive array of protic and aprotic solvents, Krawczyk (1989) arrived at the following *empirical* relationship between the shift in λ_Q and $\nu_{C=O}$:

$$\Delta\lambda_Q = 0.23(1686.7 - \nu_{C=O}) \quad (5)$$

In Krawczyk's formalism, $\Delta\lambda_Q$ is the shift in wavelength that occurs exclusively by hydrogen bonding, after medium dielectric effects are taken into account. Equation 5 states that in the limit of no hydrogen bonding to the C_9=O group, $\nu_{C=O} > 1686.7$ cm^{-1}. This is of great help in describing chlorophyll–protein interactions in CP47, as will be shown below.

When applied judiciously, eq 5 allows us to use vibrational data to estimate the electronic properties of hydrogen-bonded chlorophylls. An added advantage is the ability to use resonance Raman spectra obtained with Soret excitation to glean insight into the highly fluorescent Q electronic state. As is shown clearly by our data, the fluorescence background intrinsic to this protein (τ_{mean} = 2.9 ns) would prevent the acquisition of Q-excited Raman spectra.

We wish to assess the relative importance of chromophore–protein interactions over excitonic interactions in determining the electronic structure of bound chlorophylls in CP47. Let us consider the population exhibiting $\nu_{C=O}$ = 1670 cm^{-1}. According to eq 5, this population is likely to be involved in hydrogen-bonding with the medium, via the C_9 keto group. Ligation of C_9=O to the Mg^{2+} ion of an adjacent chlorophyll may be dismissed because the $\nu_{C=O}$ value observed in CP47 is some 15 cm^{-1} too high for this kind of interaction (Lutz, 1974; Koyama et al., 1986).

Equation 5 states that hydrogen bonding alone can account for a 3.8-nm shift in λ_Q for this population. This value of $\Delta\lambda_Q$ is only approximate because our experiments were conducted at low temperature, whereas the data used to establish the relationships of eq 5 were obtained at room temperature (Krawczyk, 1989). Nonetheless, our result is significant because the Q bands of functional chlorophyll states in CP47 are separated by only a few nanometers (van Dorssen et al., 1987): the largest separation is 23 nm (691 nm – 668 nm) and the smallest is 9 nm (677 nm – 668 nm). We conclude from this calculation that changes in the electronic structure of chlorophyll *a* caused by hydrogen-bonding interactions at the C_9 keto group are not negligible relative to other interactions that may contribute to the separation of the Q_y(0–0) bands. Consequently, hydrogen bonding and excitonic interactions together play key roles in optimizing those parameters involved in Förster energy transfer, such as spectral overlap (Förster, 1959).

Whereas our current study has provided useful insight on the role of chlorophyll–protein interactions in excitation energy transfer, a quantitative treatment of excitonic interactions has not been attempted. We hope that the analysis of the Raman excitation profiles of the $\nu_{C=O}$ bands, underway in our laboratory, will address this issue successfully.

ACKNOWLEDGMENT

We thank Professor Warren F. Beck (Vanderbilt University) for useful discussions.

REFERENCES

Akabori, K., Tsukamoto, H., Tsukihara, J., Nagatsuka, T. Motokawa, O., & Toyoshima, Y. (1988) *Biochim. Biophys. Acta 932*, 345–357.

Alcala, J. R., Gratton, E., & Prendergast, F. G. (1987) *Biophys. J. 51*, 597–604.

Booth, P. J., Crystall, B., Ahmad, I., Barber, J., Porter, G., & Klug, D. R. (1991) *Biochemistry 30*, 7573–7586.

Bricker, T. M. (1990) *Photosynth. Res. 24*, 1–13.

Brown, R. G., Evans, E. H., Holderness, S. G., Manwaring, J., & May, B. (1983) *Photobiochem. Photobiophys. 5*, 87–92.

Connolly, J. S., Janzen, A. F., & Samuel, E. B. (1982) *Photochem. Photobiol. 36*, 559–563.

Crystall, B., Booth, P. J., Klug, D. R., Barber, J., & Porter, G. (1989) *FEBS Lett. 249*, 75–78.

Deisenhofer, J., & Michel, H. (1991) in *The Chlorophylls* (Scheer, H., Ed.) Chapter 3.5, pp 613–625, CRC Press, Boca Raton, FL.

Dekker, J. P., Bowlby, N. R., & Yocum, C. F. (1989) *FEBS Lett. 254*, 150–154.

de Paula, J. C.,, Ghanotakis, D. F., Bowlby, N. R., Dekker, J. P., Yocum, C. F., & Babcock, G. T. (1990) in *Current Research in Photosynthesis* (Baltscheffsy, M., Ed.), Vol. I, pp 643–646, Kluwer Academic Publishers, Dordrecht, The Netherlands.

de Paula, J. C., Walters, V.A., Hall, K., Lind, J., & Nutaitis, C. (1992) *J. Phys. Chem. 96*, 10591–10594.

de Vitry, C., Wollmann, F.-A., & Delepelaire, P. (1984) *Biochim. Biophys. Acta 767*, 415–422.
Durrant, J. R., Giorgi, L. B., Barber, J., Klug, D. R., & Porter, G. (1990) *Biochim. Biophys. Acta 1017*, 167–175.
Förster, T. (1959) *Discuss. Faraday Soc. 27*, 7–17.
Fujiwara, M., & Tasumi, M. (1986) *J. Phys. Chem. 90*, 250–255.
Ghanotakis, D. F., & Yocum, C. F. (1986) *FEBS Lett. 197*, 244–248.
Ghanotakis, D. F., de Paula, J. C. Demetriou, D. M., Bowlby, N. R., Petersen, J., Babcock, G. T., & Yocum, C. F. (1989) *Biochim. Biophys. Acta 974*, 44–53.
Govindjee, van de Ven, M., Preston, C., Seibert, M., & Gratton, E. (1990) *Biochim. Biophys. Acta 1015*, 173–179.
Hansson, Ö., Duranton, J., & Mathis, P. (1988) *Biochim. Biophys. Acta 932*, 91–96.
Hastings, G., Durrant, J. R., Barber, J., Porter, G., & Klug, D. R. (1992) *Biochemistry 31*, 7638–7647.
Hawthorthwaite, A. M., & Cogdell, R. J. (1991) in *The Chlorophylls* (Scheer, H., Ed.) Chapter 3.1, pp 493–528, CRC Press, Boca Raton, FL.
Hoff, A. J., & Amesz, J. (1991) in *The Chlorophylls* (Scheer, H., Ed.) Chapter 4.1, pp 723–738, CRC Press, Boca Raton, FL.
Holtom, G. R. (1990) in *Time-Resolved Laser Spectroscopy in Biochemistry II*, SPIE Proceedings Series, Vol. 1204, pp 2–12, Bellingham, WA.
Kobayashi, M., Maeda, H., Watanabe, T., Nakane, H., & Satoh, K. (1990) *FEBS Lett. 260*, 138–140.
Koyama, Y., Umemoto, Y., Akamatsu, A., Uehara, K., & Tanaka, M. (1986) *J. Mol. Struct. 146*, 273–287.
Krawczyk, S. (1989) *Biochim. Biophys. Acta 976*, 140–149.
Lutz, M. (1974) *J. Raman Spectrosc. 2*, 497–516.
Lutz, M., & Robert, B. (1988) in *Biological Applications of Raman Spectroscopy* (Spiro, T. G., Ed.) Vol. 3, pp 347–411, J. Wiley & Sons, New York.
Lutz, M., & Mäntele, W. (1991) in *The Chlorophylls* (Scheer, H., Ed.) Chapter 4.6, pp 855–902, CRC Press, Boca Raton, FL.
McCauley, S. W., Baronavski, A. P., Rice, J. K., Ghirardi, M. L., & Mattoo, A. K. (1992) *Chem. Phys. Lett. 198*, 437–442.
Mimuro, M., Yamazaki, I., Itoh, S., Tamai, N., & Satoh, K. (1988) *Biochim. Biophys. Acta 933*, 478–486.
Möenne-Loccoz, P., Robert, B., & Lutz, M. (1989) *Biochemistry 28*, 3641–3645.
Nanba, O., & Satoh, K. (1987) *Proc. Natl. Acad. Sci. U.S.A. 84*, 109–112.
Petersen, J., Dekker, J. P., Bowlby, N. R., Ghanotakis, D. F., Yocum, C. F., & Babcock, G. T. (1990) *Biochemistry 29*, 3226–3231.
Roelofs, T. A., Gilbert, M., Shuvalov, V. A., & Holzwarth, A. R. (1991) *Biochim. Biophys. Acta 1060*,, 237–244.
Sundström, V., & van Grondelle, R. (1991) in *The Chlorophylls* (Scheer, H., Ed.) Chapter 5.1, pp 1097–1124, CRC Press, Boca Raton, FL.
Takahashi, Y., Hansson, Ö., Mathis, P., & Satoh, K. (1987) *Biochim. Biophys. Acta 893*, 49–59.
Tang, D., Jankowiak, R., Seibert, M., & Small, G. (1991) *Photosynth. Res. 27*, 19–29.
Tasumi, M., & Fujiwara, M. (1987) in *Spectroscopy of Inorganic-Based Materials* (Clark, R. J., H., & Hester, R. E., Eds.) Chapter 6, pp 407–428, John Wiley & Sons, New York.
Thibodeau, D. L., & Koningstein, J. A. (1989) *J. Phys. Chem. 93*, 7713–7717.
Thompson, L. K., & Bridvig, G. W. (1988) *Biochemistry 27*, 6653–6658.
Thornber, J. P., Morishige, D. T., Anandan, S., & Peter, G. F. (1991) in *The Chlorophylls* (Scheer, H., Ed.) Chapter 3.3, pp 549–585, CRC Press, Boca Raton, FL.
Trautman, J. K., Shreve, A. P., Violette, C. A., Frank, H. A., & Owens, T. G. (1990) *Proc. Natl. Acad. Sci. U.S.A. 87*, 215–219.
Van Dorssen, R. J., Breton, J., Plijter, J. J., Satoh, K., Van Gorkom, H. J., & Amesz, J. (1987) *Biochim. Biophys. Acta 893*, 267–74.
Vermaas, W. F. J., Williams, J. G. K., & Arntzen, C. J. (1987) *Plant Mol. Biol. 8*, 317–326.
Wasielewski, M. R., Johnson, D. G., Seibert, M., & Govindjee (1989a) *Proc. Natl. Acad. Sci. U.S.A. 86*, 524–528.
Wasielewski, M. R., Johnson, D. G., Govindjee, Preston, C., & Seibert, M. (1989b) *Photosynth. Res. 22*, 89–99.